International Journal of Thermophysics, Vol. 1, No. 4, 1980

Correlation of the Transport Properties of Simple Fluids at Low Temperatures and High Pressures Based on the Generalized Eucken Relation and the Molecular Dynamics of Hard Sphere Fluid

T. H. Chung,[1] L. L. Lee,[1] and K. E. Starling[1]

Received May 12, 1980

A generalized correlation is developed for the viscosity and thermal conductivity of isotropic fluids under high pressures (up to 200 MPa) and low temperatures (down to 85 K). Two known observations have been taken into consideration in the development of the correlation. First, the Alder correction factors for the Enskog theory values of transport coefficients obtained from molecular dynamics simulations for hard sphere fluids are incorporated. The inclusion of these corrections in the theory makes it possible to describe correctly the density dependence of the hard sphere viscosity and thermal conductivity at high pressures. The hydrodynamic "cage" effect, which is manifested in the molecular motions of dense fluid systems, is thus correctly accounted for. Second, the generalized Eucken relation, which relates the thermal conductivity to the viscosity, is incorporated. As a consequence, an internally consistent correlation is obtained, which can adequately predict the behavior of the thermal conductivity from given values of viscosity. Tests on simple fluids, such as argon, krypton, etc., show that the correlation is valid within a few percent for the entire fluid range where experimental data are available for comparison, and also along the vapor–liquid saturation line, with the exclusion of the critical region. Furthermore, since the variables appearing in the theory are in reduced form, a corresponding states correlation is established for isotropic fluids.

KEY WORDS: viscosity; thermal conductivity; Enskog theory; diffusion coefficient; Eucken relation.

1. INTRODUCTION

Recent developments in the computer simulation (e.g., molecular dynamics) of model systems in statistical mechanics have shed much light on the

[1]School of Chemical Engineering and Materials Science, University of Oklahoma, Norman, Oklahoma 73019, U.S.A.

0195-928X/80/1200-0397$03.00/0

detailed behavior and dynamics of transport processes. One prominent example is the work of Alder et al. [1] for hard sphere molecular dynamics. Alder et al. have shown that at high densities, the Enskog results for the diffusion coefficient, viscosity, and thermal conductivity are inadequate. Examination of the trajectories of the hard spheres showed vortex motions at medium densities. The now well-known "cage effect" was observed at high densities, i.e., each hard sphere is situated in the center of a "cage" formed by its neighbors, and its forward motion is deflected at short molecular distances to give a backward scattering. This explains the negativity of the velocity autocorrelation function at intermediate times, which is present at high densities, but not at low densities where no "cage" exists. This high density effect is not restricted to hard sphere fluids; in fact, the same phenomenon was discovered for Lennard-Jones molecules and diatomic molecules. Therefore, the Enskog theory must be revised in order to explain the transport behavior of dense fluids.

One revision of the Enskog theory presented previously is the so-called MET (Modified Enskog Theory) of Hanley et al. [2]. This theory is valid up to about twice the critical density for argon and methane. Attempts have been made to utilize the Alder hard sphere results in the prediction of real fluid properties. In engineering applications, Gotoh [3] has used the corrected Enskog diffusion coefficient for polyatomic molecules. Protopapas et al. [4] applied the Alder correction factor to the case of liquid metals. Dymond [5] made an integral formulation of the effects of Alder's correction and applied it to the diffusion coefficient of carbon tetrachloride. Woolf [6] applied it to water, and Chandler [7] added rotational contributions for polyatomic molecules. Harris [8] discussed Chandler's formulation for the methane diffusion coefficient.

In this paper, we present a general and consistent method of utilizing the molecular dynamics results together with the theoretical interrelations among the transport properties to predict dense real fluid behavior. The method is general, in that wide temperature and pressure ranges are included. The resultant correlation is self-consistent, since all three transport properties are interrelated through the Stokes-Einstein and Eucken relations.

In Section 2, we review the Enskog theory for transport properties. In Section 3, the diffusion coefficient of argon is predicted based on the corrected hard sphere model. This is made possible through a temperature dependent hard sphere diameter, d_B. In Section 4, we calculate the viscosity of isotropic fluids via the generalized Stokes–Einstein relation. Close agreement with extensive experimental data sources is achieved. The thermal conductivity is calculated from the generalized Eucken relation in Section 5. Comparison with argon, krypton, and xenon data shows validity of the method over wide ranges of temperatures and pressures.

2. ENSKOG THEORY

We first review the Enskog equations for transport coefficients. The self-diffusion coefficient, D_E, given by Enskog for dense fluid hard spheres, is

$$D_E = D_0/\chi \tag{1}$$

where D_0 is the dilute gas self-diffusion coefficient,

$$D_0 = 3/8\ (\rho m)^{-1}\ (\pi mkT)^{1/2}/\pi d^2\Omega^{(1,1)*} \tag{2}$$

where $\Omega^{(1,1)*}$ is the collision integral, which for hard spheres is unity, χ is the contact value of the hard sphere radial distribution function (rdf), ρ is the molecule number density of the fluid, m is the mass per molecule, k is the Boltzmann constant, T is the absolute temperature, and d is the diameter of the hard spheres.

The equation for the Enskog viscosity η_E is given by the relation

$$\eta_E = \eta_0 b\rho[(b\rho\chi)^{-1} + 0.800 + 0.761\ b\rho\chi] \tag{3}$$

where b is related to the second virial coefficient of hard spheres and is given by

$$b = 2/3\ \pi d^3 \tag{4}$$

and η_0 is the dilute gas viscosity for hard spheres,

$$\eta_0 = 5/16\ (\pi mkT)^{1/2}/\pi d^2 \tag{5}$$

The Enskog thermal conductivity, λ_E, is given by

$$\lambda_E = \lambda_0 b\rho[(b\rho\chi)^{-1} + 1.200 + 0.755\ b\rho\chi] \tag{6}$$

where λ_0 is the dilute gas thermal conductivity,

$$\lambda_0 = \frac{25}{32m}\frac{(\pi mkT)^{1/2}\,C_v^0}{\pi d^2} \tag{7}$$

where $C_v^0 = (3/2)k$.

3. THE SELF-DIFFUSION COEFFICIENT

The validity of the Enskog self-diffusion coefficient for dense hard sphere fluids has recently been tested by the molecular dynamics simulation

of Alder et al. [1]. Equation (1) was found to be inadequate at moderately high densities. The "exact" hard sphere self-diffusion coefficient, D, is related to the Enskog value, D_E, by a correction coefficient, C_D, which is a function of density,

$$D = C_D \cdot D_E \tag{8}$$

The behavior of C_D as a function of density is given in Fig. 1. It is seen that at low densities ($\rho d^3 \lesssim 0.2$), C_D is very close to unity. At intermediate densities ($0.2 \lesssim \rho d^3 \lesssim 0.78$), C_D reaches 1.34, representing an enhancement of the diffusive processes over the Enskog values. At much higher densities

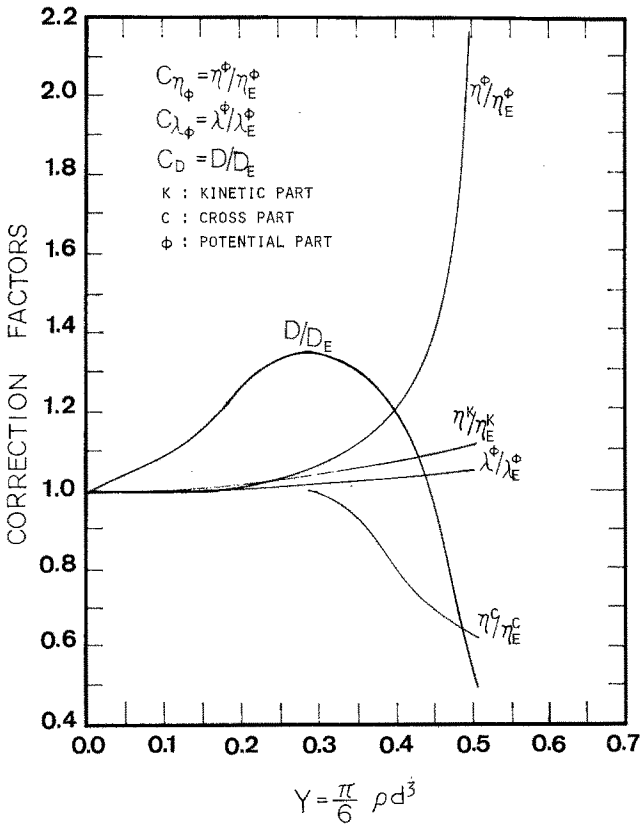

Fig. 1. Correction factors of the Enskog transport coefficients for hard spheres. D, diffusion coefficient; η, viscosity; λ, thermal conductivity; subscript E, Enskog values. (From Alder et al. [1].)

($\rho d^3 \gtrsim 0.85$), C_D drops down to values less than unity; e.g., $C_D = 0.58$ at $\rho d^3 = 0.943$. This is due to the so-called "cage" effect, which was absent from the Enskog approach. Therefore, we found that the density variation of the self-diffusion coefficient for hard spheres is of a quite complicated nature, which cannot be accounted for by the Enskog solution. Since the elucidation of Alder's work, the correction factor C_D has received wide attention in both theoretical and correlational work (Gotoh, [3]). We shall also exploit the Alder correction in our correlation here.

Based on the Alder correction factor, C_D, the hard sphere self-diffusion coefficient is now given by

$$D = C_D \cdot D_E = 3/8 \frac{(kT/\pi m)^{1/2}}{d^2 \rho \chi} \cdot C_D \tag{9}$$

Alternatively,

$$\frac{\rho^* D^*}{(\rho^* D^*)_0} = 4\xi \frac{C_D}{Y_{HS}} \tag{10}$$

where ξ is the packing fraction for hard spheres,

$$\xi = \pi/6 \, \rho d^3 \tag{11}$$

where ρ is the number density, and Y_{HS} is the internal pressure,

$$Y_{HS} = \frac{1 + \xi + \xi^2 - \xi^3}{(1 - \xi)^3} - 1 \tag{12}$$

Equation (10) reproduces the molecular dynamics results for hard spheres. But real fluids are not composed of hard sphere molecules. To generalize Eq. (10) to real fluids, or at least to monatomic and isotropic fluids, we can follow either the procedure of Hanley and Cohen [9] in their MET theory to require

$$Y = T \frac{\delta Z}{\delta T}\bigg|_v + Z - 1 \tag{13}$$

or adopt the conformal solution theory concept using the hard spheres as reference fluid (Frisch and McLaughlin [10]) and represent the real fluid behavior by a hypothetical fluid with hard sphere equivalent diameter, d_B. The basis for such an approach lies in the observation that the velocity

autocorrelation functions (*vcf*), whereby the self-diffusion coefficient is derived, show for real fluids the same density variation effects as for hard spheres (see, e.g., the Lennard-Jones *vcf* of Levesque et al. [11], or even the diatomic *vcf* of Evans and Streett [12]. Levesque and Verlet [13] have shown that for the Lennard-Jones fluid, the Alder correction factor improves the Enskog values for diffusion coefficient and viscosity. Most simulation results for simple molecules show the same "cage" effects at high densities and a certain degree of enhancement of the diffusion coefficient at medium densities, similar to the hard sphere fluid.

For the noble gases, the Lennard-Jones potential gives a reasonable description at moderate densities and temperatures. To predict the diffusion coefficients of argon, we used Eqs. (10), (11), and (12) and compared the results with the molecular dynamics results for Lennard-Jones molecules. We determined the equivalent hard sphere diamter d_B from fitting the *MD* results of Levesque and Verlet [13] and Michels and Trappeniers [14]. The following temperature-dependent equation for d_B is obtained:

$$d_B = \frac{1.91 + 1.09857\beta}{2.10754 + \beta} \tag{14}$$

where $\beta = 1/T^*$, $T^* = kT/\epsilon$, and d_B is measured in the units of σ, with σ the Lennard-Jones distance parameter, and ϵ the *LJ* energy parameter (see Table I). With d_B determined from Eq. (14), we calculate ξ and Y_{HS} from Eqs. (11) and (12), respectively, replacing the diameter d by d_B. These values are in turn used in Eq. (10) for the calculation of the diffusion coefficient (ρD). For the dilute state, $(\rho D)_0$ of argon or krypton, Eq. (2) is used with the collision integral $\Omega^{(1,1)*}$ evaluated for the LJ potential. The results of such calculation for argon are shown in Fig. 2. Both the experimental argon self-diffusion coefficient and *MD* simulation values are shown. It is seen that at high densities, Eq. (10), with d_B from Eq. (14), gives a good description of the self-diffusion coefficient of argon. At low densities, there is an artificial "rippling" effect due to the fit; see Eq. (14). Also, the simulation numbers of Michels and Trappeniers [14] are not consistent enough (especially in the temperature trend of the diffusion coefficient) to give a good resolution of the

Table I. Potential Parameters

Substance	ϵ/k (K)	σ (Å)
Ar	119.80	3.405
Kr	166.28	3.641
Xe	230.05	3.968

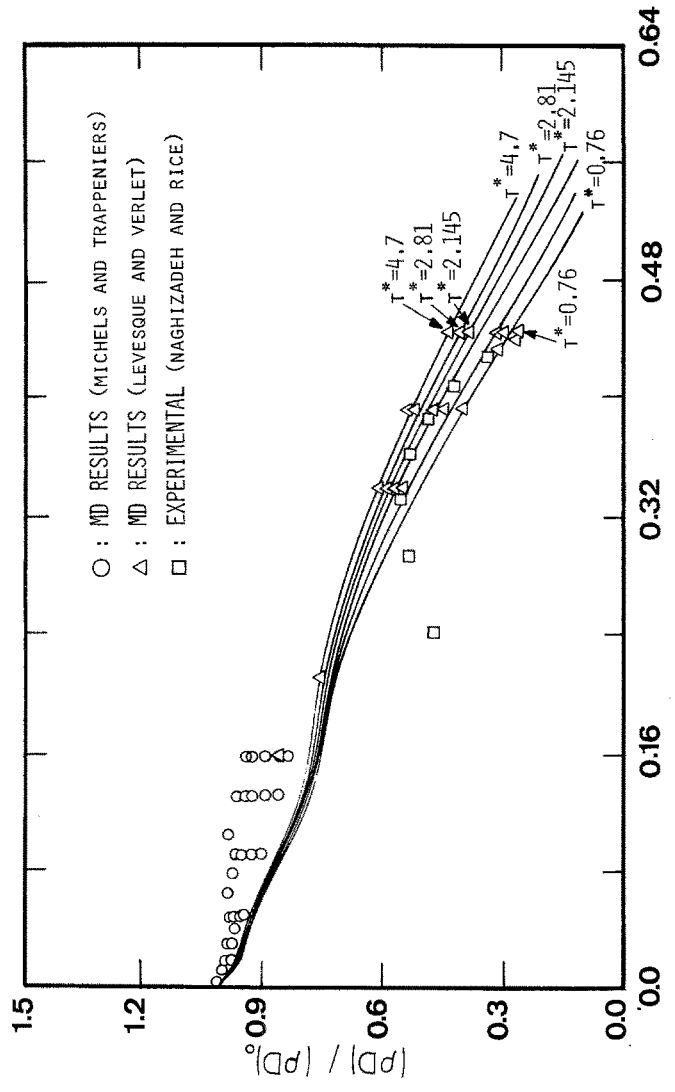

Fig. 2. Comparison of the diffusion coefficients of the Lennard-Jones fluid. Molecular dynamics results: Δ, Levesque and Verlet [13]; ○, Michels and Trappeniers [14]; solid lines, our calculations. Squares are experimental argon data.

Table II. Self-Diffusion Coefficient of Saturated Liquid Argon[a]

T (K)	P (bar)	$D_{calc} \times 10^6$ m^2/s	$D_{expt.} \times 10^6$ m^2/s
90	1.34	22.20	24.30
100	3.25	30.63	35.40
110	6.68	41.04	48.00
120	12.14	54.15	60.60
130	20.26	72.39	74.50
140	31.72	100.87	87.20
150	47.42	149.13	99.80

[a]From Naghizadeh and Rice [41].

fit (to within 6.5% AAD, average absolute deviation). The prediction of the experimental self-diffusion coefficient of argon is given in Table II. The Levesque and Verlet [13] molecular dynamics results were fitted with an error of 4.3% AAD.

We note that the ratio $(\rho D)/(\rho D)_0$ is temperature dependent as well as density dependent. The dependence on temperature is small compared to the density dependence. However, as will be seen later, this temperature trend is important in the viscosity prediction, if correct viscosity variation with temperature is to be achieved.

4. VISCOSITY

Recall that the Enskog viscosity for dense hard sphere fluids is

$$\eta_E = \eta_0 b\rho \left[\frac{1}{b\rho\chi} + 0.800 + 0.761\, b\rho\chi\right] \tag{15}$$

which is of the form

$$\eta = \eta_k + \eta_c + \eta_\phi \tag{16}$$

when Eq. (15) is multiplied through, the first term on the right-hand side is the kinetic contribution, η_k, the second term is the cross contribution (from interaction of kinetic and potential effects), η_c, and the third term is the potential contribution, η_ϕ. Mo and Starling [15] have derived an interrelationship between the self-diffusion coefficient D and the potential contribution η_ϕ, corresponding to the so-called Stokes-Einstein relation,

$$\eta_\phi^* = A_5 \frac{Y^2 T^*}{\rho^* D^*} \tag{17}$$

where A_5 is a constant determined from data, T^* is the reduced temperature, $T^* = kT/\epsilon$, ρ^* is the reduced density, $\rho^* = \rho\sigma^3$, D^* is the reduced self-diffusion coefficient, where $D = D^*\sigma\,(\epsilon/m)^{1/2}$, $Y = (\pi/6)\,\rho\sigma^3$, and η_ϕ^* is the potential contribution to the viscosity in reduced form. The reduced viscosity, η^*, is defined by the relation

$$\eta^* = \left[26.693\,\frac{\sqrt{M\epsilon/k}}{\sigma^2}\right]^{-1}\eta \tag{18}$$

where M is molecular weight, and the units used are η in μp, ϵ/k in Kelvins, and σ in Å. To calculate (ρ^*D^*) for dense fluids, we can use the corrected Alder-Enskog expression, Eq. (10). We need an expression for the quantity $(\rho D)_0$ for real dilute gases. We adopt the formula for Lennard-Jones gases from Hirschfelder et al. [16] with the second-order Sonine correction,

$$(\rho^*D^*)_0 = 0.21156\,\frac{T^{*1/2}}{\Omega^{(1.1)*}}\cdot\frac{1}{1-\Delta} \tag{19}$$

where

$$\Delta = \frac{[6C^* - 5)^2}{(55 - 12B^* + 16A^*)} \tag{20}$$

A^*, B^*, and C^* are given by the following relations:

$$\begin{aligned} A^* &= \Omega^{(2,2)*}/\Omega^{(1,1)*} \\ B^* &= [5\Omega^{(1,2)*} - 4\Omega^{(1,3)*}]/\Omega^{(1,1)*} \\ C^* &= \Omega^{(1,2)*}/\Omega^{(1,1)*} \end{aligned} \tag{21}$$

We note that ϵ and σ are the LJ parameters for the monatomic gases. Their values for argon, krypton, and xenon are given in Table I. In Eqs. (19), (20), and (21), the collision integrals for the LJ potential tabulated by Hirschfelder et al. [16] are used.

The remaining contributions to the viscosity, η_k and η_c, are approximated by the formula

$$\eta_k^* + \eta_c^* = \eta_0^*\left[\frac{1}{C(Y)} + A_4\,Y\right] \tag{22}$$

where

$$C(Y) = 1 + A_6 Y + A_7 Y^2 \tag{23}$$

The dilute gas viscosity, η_0^* for the Lennard-Jones fluid, is given by the relation

$$\eta_0^* = T^{*1/2} / \Omega^{(2,2)*} \tag{24}$$

However, it is known that for monatomic gases, Eq. (24) is not accurate at high temperatures. A correction factor $f(T^*)$ therefore is applied, i.e.,

$$\eta_0^* = T^{*1/2} \cdot f(T^*) / \Omega^{(2,2)*} \tag{25}$$

where

$$f(T^*) = A_1 + A_2 T^* + A_3 T^{*2} \tag{26}$$

The complete expression for the reduced viscosity, η^*, is then

$$\eta^* = \eta_0^* \left[1/C(Y) + A_4 Y \right] + A_5 \frac{Y^2 T^*}{\rho^* D^*} \tag{27}$$

Several points can be noted with respect to Eq. (27). First, it contains all three parts of the viscosity, i.e., the kinetic part, η_k^*, involving the reciprocal C-function, the cross part, η_c^*, involving $A_4 Y$, and the potential part, η_ϕ^*, given by the term with coefficient A_5. Second it utilizes the Stokes–Einstein relation to connect the potential part of the viscosity with self-diffusion coefficient via Eq. (17). Third, the good results obtained in Sec. 3 for the self-diffusion coefficient can now be utilized to obtain the viscosity. This approach makes maximum use of the simulation results for dense hard spheres, incorporating the vortex effects at high densities, and connects molecular dynamics to the theoretical interrelationship as given by the generalized Stokes–Einstein equation (17) to forge a complete model for viscosity.

The constants A_i used for the monatomic fluids were determined from fitting Eq. (27) to argon, krypton, and xenon data over wide ranges of temperatures and pressures. Their values are given in Table III. It is noted that in order to use Eq. (27), the value of density is needed given the experimental conditions. Some experiments reported the densities along with the temperatures and pressures, whereby the experimental densities were chosen in the correlation. For cases where only temperatures and pressures were given, the densities were calculated from an accurate equation of state in the form of Gosman et al. [17] (see also, Twu et al. [18]).

Figures 3 and 4 show the fit to argon experimental viscosity. Figure 3 shows three isotherms at 107.7 139.7, and 298 K. The density range covers dilute to dense states near the triple point ($\rho^* \simeq 0.85$). It is seen that the calculated values follow the experimental data remarkably well at high densities even for the lowest temperature (107.7 K). We note that the reduced residual viscosity $\eta^* - \eta_0^*$ decreases with increasing temperature at constant density, while the diffusivity ratio, $(\rho^* D^*)/(\rho^* D^*)_0$ increases with increasing temperature. Since the quantity $(\rho^* D^*)$ appears in the denominator of Eq. (27), the correct trend is obtained. In Fig. 4, where all the data points used in the correlation are shown, similar agreement is evident.

Table IV exhibits the detailed comparison of the calculated viscosity values with data from different experimental sources. For example, the comparison with the NBS data for Ar (Haynes [19]) shows an AAD of less than 1% for 166 data points covering temperatures from 85 to 298 K and pressures from low pressures to 34 MPa. There were 93 data from Michela et al. [21], covering pressures from 927 kPa to 201 MPa and temperatures from 273 to 348 K. Our prediction is within 2.8% AAD. A total of 517 experimental data from 14 sources were compared. For most data sources, the agreement is within 1–2% AAD. The greatest discrepancy comes from Hellemans et al. [27] (5.4% AAD). Agreement with the results of Kestin et al. [24, 25], Kestin and Leidenfrost [29], and DiPippo and Kestin [22] is generally good (0.5, 0.7, 0.8, and 0.2% AAD for pressures up to 10 MPa and temperatures from 293 to 973 K).

For krypton, predicted viscosities were compared with 72 data points. The results were 0.4% AAD agreement with the data of Kestin and Leidenfrost [29] (101 kPa to 2.16 MPa, at 293.15 K) and 0.8% agreement with the data of Reynes and Thodos [28] (at pressures up to 83 MPa and temperatures

Table III. Values of Parameters for Use with Viscosity and Thermal Conductivity Correlations

i	A_i^a
1	0.962387
2	0.133183×10^{-1}
3	-0.503944×10^{-3}
4	−0.796386
5	3.483350
6	−2.375940
7	7.424750
8	0.754815
9	0.927051
10	0.381552
11	-0.321260×10^{-1}

[a]See Eqs. (27), (32), and (33.).

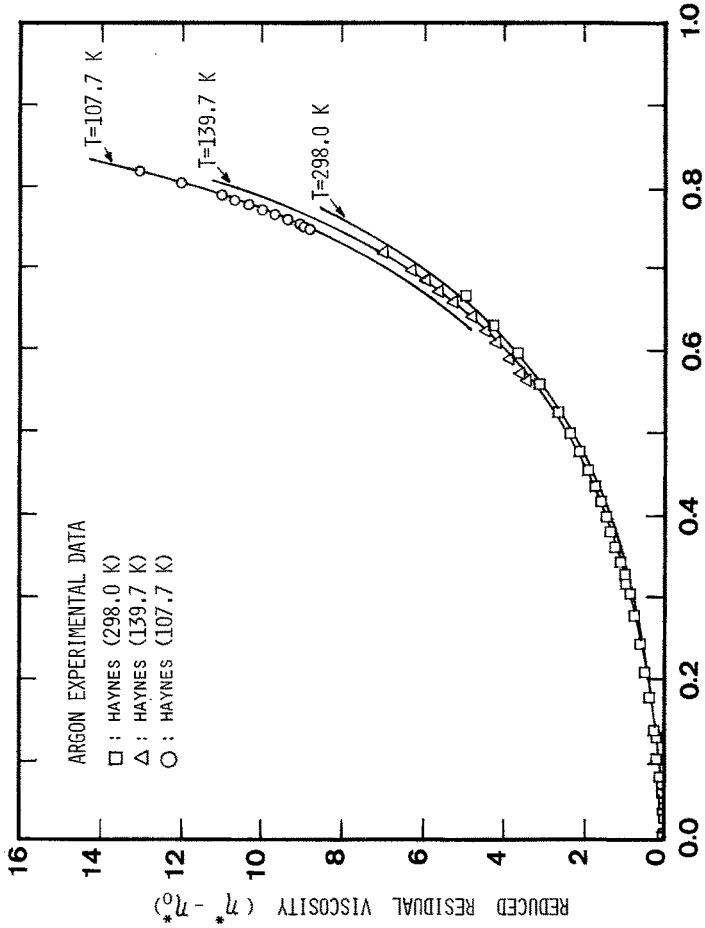

Fig. 3. Viscosity of argon along three isotherms: T = 107.7 K (○), 139.7 K (△), and 298 K (□). Solid lines, calculated values.

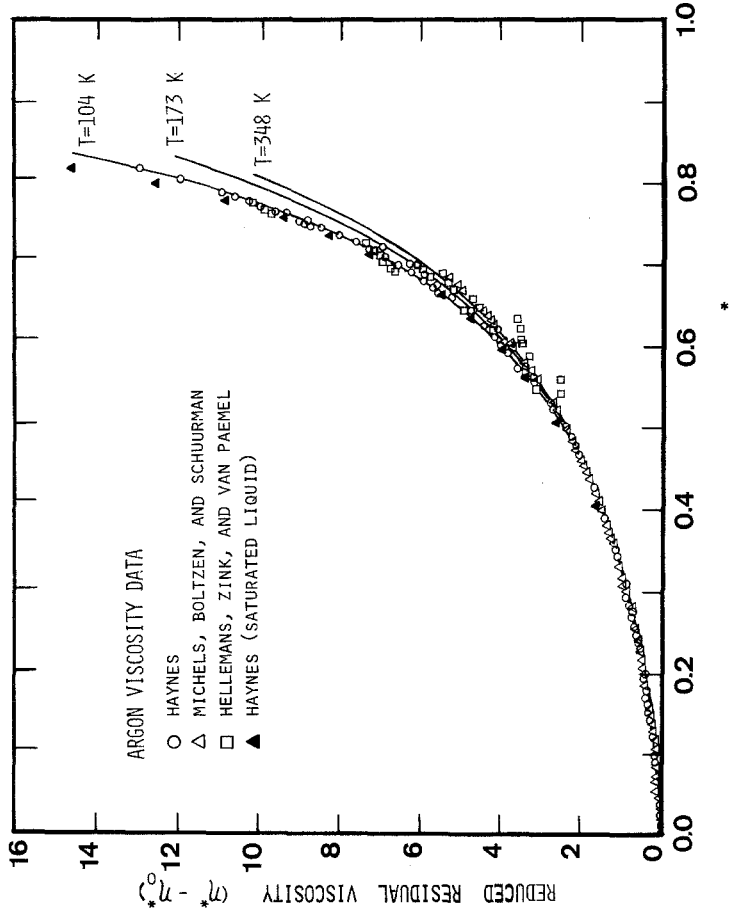

Fig. 4. The variation of the residual viscosity of argon with reduced density. Points, experimental results; solid lines, calculated values.

Table IV. Calculation Results for Viscosity

Fluid	Data points	Temperature range (K)	Pressure range (bar)	Density range (kg/m^3)	Avg. abs. dev. (%)	Max. dev. (%)	Reference
Argon	166	85.0–298.0	0.69–345.12	2.6–1407.7	0.97	5.84	Haynes [19]
	43	173.2–298.2	4.60–170.92	10.0–837.6	0.78	1.68	Gracki et al. [20]
	93	273.0–348.0	9.27–2,019.45	16.4–1,135.2	2.80	5.36	Michels et al. [21]
	23	297.5–575.2	0.30–1.76	0.3–2.6	0.22	0.79	DiPippo and Kestin [22]
	26	194.7–373.2	29.21–188.47	47.9–693.0	1.05	2.66	Flynn et al. [23]
	40	297.8–298.5	1.01–101.4	1.7–171.5	0.54	0.75	Kestin et al. [24]
	7	373.2–973.2	1.01	0.5–1.3	0.66	1.50	Kestin et al. [25]
	21	1,100.0–2,100.0	1.01	0.2–0.4	0.18	0.42	Guevara et al. [26]
	33	104.5–141.1	4.66–98.08	923.4–1321.4	5.35	22.92	Hellemans et al. [27]
	35	373.2–473.2	71.36–829.77	71.0–716.7	1.67	4.39	Reynes and Thodos [28]
	15	293.1–298.2	0.39–31.22	1.2–52.2	0.78	0.84	Kestin and Leidenfrost [29]
	5	84.1–86.9	1.01	1,403.9–1,420.8	1.96	2.60	Saji and Kobayasi [30]
	4	84.2–87.3	1.01	1,403.1–1,423.1	2.51	3.77	Van Itterbeek and Van Paemel [31]
	6	83.9–89.0	1.01	1,402.0–1,433.0	2.81	4.04	Boon et al. [32]
Krypton	20	303.9–472.6	0.41–1.74	2.2–5.8	1.48	4.07	DiPippo and Kestin [22]
	6	293.2–293.2	1.01–21.67	3.5–78.3	0.43	0.96	Kestin and Leidenfrost [29]
	36	373.2–473.2	71.36–830.48	152.0–1,553.0	0.76	0.97	Reynes and Thodos [28]
	10	116.1–123.0	1.01	2,399.0–2,452.0	0.49	0.96	Boon et al. [32]
Xenon	9	163.3–168.9	1.01	2,907.2–2,944.0	1.21	2.11	Legros and Thomaes [33]
	48	323.2–473.2	71.36–830.48	247.0–2,550.0	3.02	9.51	Reynes and Thodos [28]
	9	163.3–168.9	1.01	2,915.0–2,952.0	0.54	1.49	Boon et al. [32]

from 273 to 423 K). The data of DiPippo and Kestin [22] are also well predicted (20 points, 1.5% AAD).

For xenon, the correlation yields 1.2% AAD when compared with the experimental viscosity data of Legros and Thomaes [33]. The original reported density conditions in the xenon data of Reynes and Thodos [28] were not correct (the same densities were reported at different temperatures). A correction of their densities was made and the calculation of viscosity agrees with the experimental results to with 3.0% AAD. For the results of Boon et al. [32], the correlation predicts viscosities with 0.5% AAD.

5. THERMAL CONDUCTIVITY

We have shown previously (Mo and Starling [15]) that a generalized Eucken relation for the interrelation between the thermal conductivity and the viscosity of monatomic fluids is

$$\lambda = \frac{15}{4}\frac{R}{M}(\eta_k + \eta_c) + (\rho D)_0(C_v^0 - 1.5R) + \frac{5}{2}\frac{R}{M}\eta_\phi - \frac{15}{8}(\eta_k + \eta_c)\frac{R}{M}\frac{\Delta H}{RT} \tag{28}$$

where R is the gas constant, C_v^0 is the dilute gas molar heat capacity at constant volume, and ΔH is the enthalpy departure from the ideal state.

In this section, we make further improvements on Eq. (28) in order to predict real gas behavior. First, we define the reduced thermal conductivity by the relation

$$\lambda^* = [19.891 \times 10^{-5} \times \sqrt{\epsilon/(Mk)}\sigma^{-2}]^{-1}\lambda \tag{29}$$

where the units of λ are cal/(cm · s · K). Then we require that

$$\lambda^* = \lambda_k^* + \lambda_c^* + \lambda_\phi^* \tag{30}$$

where

$$\lambda_k^* + \lambda_c^* = (\eta_k^* + \eta_c^*) + 1.512\,(\rho^* D^*)_0\,(C_v^{0*} - 1.5) \tag{31}$$

and

$$\lambda_\phi^* = B_1\,(2/3)\eta_\phi^*\frac{C_{\lambda\phi}}{C_{\eta\phi}} - A_8\,(1/2)\,(\eta_k^* + \eta_c^*)\,\Delta H^* \tag{32}$$

with

$$B_1 = A_9 + A_{10}\,T^* + A_{11}T^{*2} \tag{33}$$

The parameters $C_{\lambda\phi}$ and $C_{\eta\phi}$ (which are functions of density) are the Alder correction factors for thermal conductivity and voscosity, respectively, where the subscript ϕ refers to the potential contribution, $C_v^{0*} = C_v^0/R$, the reduced dilute gas specific heat, and $\Delta H^* = \Delta H/RT$, the reduced enthalpy departure. The latter can be calculated from the equation of state (Gosman et al. [17]; Twu et al. [18]). The empirical parameters A_i are given in Table III.

Equation (30), (31), and (32) were applied for the calculation of the thermal conductivity of argon, krypton, and xenon. Data for argon are relatively plentiful. For argon, a total of 643 experimental data points from six sources were investigated. The temperature range covers 90 to 1500 K, with a pressure range from 101 kPa to 245 MPa. Figure 5 shows the comparison of calculated values (continuous curves) with experimental data (symbols). It is seen that for the whole reduced density range (0.0–0.8 in $\rho\sigma^3$), the agreement is quite close. For example, there are thermal conductivity data for the whole range of densities at $T = 298.5$ K. The predicted thermal conductivities agree with the experimental data very closely for the entire density range.

Table V gives the comparison of the calculated thermal conductivity with the experimental values from different data sources for argon, krypton, and xenon. The argon data of Michels et al. [34] were fit with 1.8% AAD (for 110 points). The experimental data of Moszynski and Singh [36] are fit with 1.9% AAD. The group of data by Hanley et al. [39] are predicted with 8.1% AAD. Since their data are along the orthobaric line, the deviation of our prediction increases as the critical point (150.86 K) is approached (29% at 150 K). Therefore, the present correlation is not recommended for conditions near the critical point. For krypton and xenon, the overall average absolute deviation is about 3%.

6. CONCLUSIONS

In this investigation, we have developed a general correlation method for the transport properties of monatomic fluids: the self-diffusion coefficient, the viscosity, and the thermal conductivity for wide ranges of state conditions. There are two important elements of the correlation: (a) the use of the Alder correction factors for the values of the Enskog transport coefficients, and (b) the generalized Stokes–Einstein and Eucken equations relating the three transport properties to one another. As a consequence, an internally consistent correlation is obtained that is able to predict adequately the behavior of

Table V. Calculation Results for Thermal Conductivity

Fluid	Data points	Temperature range (K)	Pressure range (bar)	Density range (kg/m^3)	Avg. abs. dev. (%)	Max. dev. (%)	Reference
Argon	110	273.8–348.4	1.11–2456.18	1.6–1266.9	1.80	4.04	Michels et al. [34]
	359	293.7–977.7	1.00–1278.35	0.6–1046.4	1.34	4.82	Le Neindre et al. [35]
	35	323.2–473.2	1.01–1,621.24	1.1–1,075.0	1.87	5.15	Moszynski and Singh [36]
	13	300.0–1,500.0	1.01	0.3–1.6	1.25	1.98	Kestin and Wakeham [37]
	114	93.3–196.1	1.01–197.59	2.5–1395.0	4.43	12.11	Ziebland and Burton [38]
	12[a]	90.0–150.0	1.34–47.39	0.7–1371.3	8.11	29.76	Hanley et al. [39]
Krypton	13	300.0–1,500.0	1.01	0.7–3.4	0.81	2.05	Kestin and Wakeham [37]
	9[a]	120.0–200.0	1.03–42.17	1507.9–2,407.6	5.65	14.44	Ho et al. [40]
	9[b]	120.0–200.0	1.03–42.17	9.0–382.8	2.19	6.65	Ho et al. [40]
Xenon	10[a]	170.0–260.0	1.34–30.84	2,120.0–2,887.4	3.14	12.36	Ho et al. [40]
	10[b]	170.0–260.0	1.34–30.84	12.8–279.3	4.21	7.32	Ho et al. [40]

[a]Saturated liquid data.
[b]Saturated vapor data.

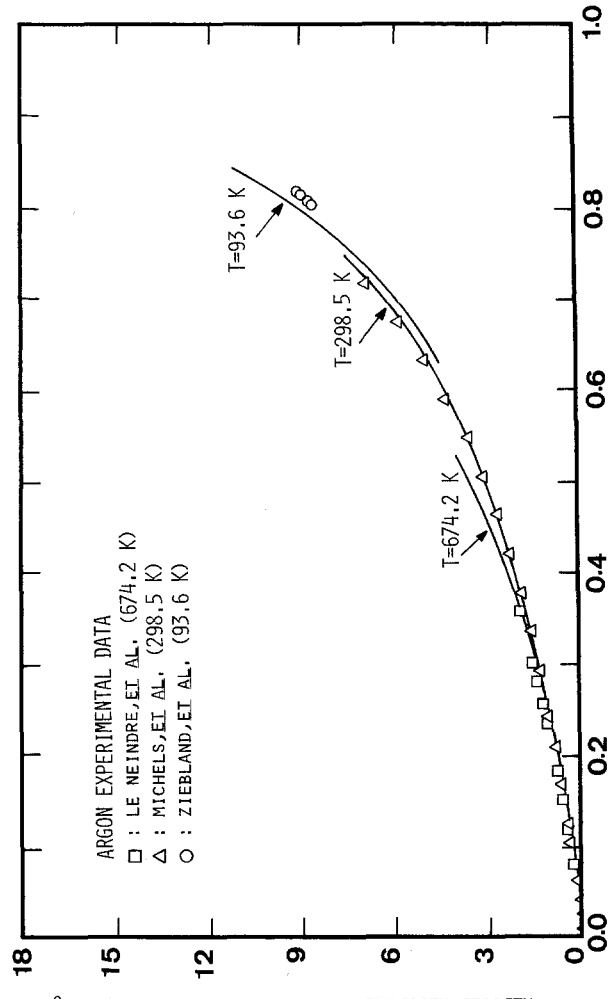

Fig. 5. The thermal conductivity of argon along three isotherms: T = 93.6 K (○), 298.5 K (△), and 674. 2 K (□). Solid lines, calculated values.

viscosity and thermal conductivity to within a few percent of the experimental values.

The temperature variations of the viscosity and thermal conductivity are correctly predicted in this framework. Examination of the experimental values of the residual viscosity, Fig. 3, and residual thermal conductivity, Fig. 5, shows that $(\partial\Delta\eta/\partial T)_\rho$ is negative and $(\partial\Delta\lambda/\partial T)_\rho$ is positive, i.e., the change in residual viscosity with respect to temperature at constant density is negative, while the opposite is true for the residual thermal conductivity. Hanley et al. [2] have given a detailed discussion on this point. This behavior seems to hold true for all normal fluids. Our theoretical equations (16), (17), (22), (30), (31), and (32) are seen to be able to give the correct trends (see Figs. 3 and 5).

The negativity of $(\partial\Delta\eta/\partial T)_\rho$ is obtained because the self-diffusion coefficient $(\rho^* D^*)$ increases with increasing temperature (Fig. 2). Consequently, η_ϕ^* decreases with increasing temperature, according to Eq. (17). The $(\partial\Delta\lambda/\partial T)_\rho$ behavior is simply due to the coefficient B_1 in Eq. (33).

In our correlation, we have not used the experimental data near the critical point. Thus our theory is not to be applied in the critical region. Examination of the self-diffusion coefficient and thermal conductivity shows that there is an abrupt change in the trend of the experimental values close to the critical point (see, e.g., Fig. 2). The source of this behavior is not clear.

One point of interest in the behavior of the residual viscosity (Fig. 4) is that at high densities the isotherms show a crossover pattern. This is clearly due to the temperature effect. One cannot treat the high density data with one temperature-independent curve. Our theory is able to distinguish the individual isotherms (Fig. 3). A plot like Fig. 4 is also good in discriminating data sources in a consistency test with other data sources.

ACKNOWLEDGMENT

We are grateful to the National Science Foundation for the support of this research under grant #ENG77-21551.

REFERENCES

1. B. J. Alder, D. M. Gass, and T. E. Wainwright, *J. Chem. Phys.* **53**:3813 (1970).
2. H. J. M. Hanley, R. D. McCarty, and E. G. D. Cohen, *Physica,* **60**:322 (1972).
3. K. Gotoh, *Ind. Eng. Chem. Fundamentals* **15**:180 (1976).
4. P. Protopapas, H. C. Andersen, and N. A. D. Parlee, *J. Chem. Phys.* **59**:15 (1973).
5. J. H. Dymond, *J. Chem. Phys.* **60**:969 (1974).
6. L. A. Woolf, *J. Chem. Phys.* **57**:3013 (1972); **61**:1600 (1974).
7. D. Chandler, *J. Chem. Phys.* **62**:1358 (1975).
8. K. R. Harris, *Physica* **94A**:448 (1978).
9. H. J. M. Hanley and E. D. G. Cohen, *Physica,* **83A**:215 (1976).

10. H. L. Frisch and E. McLaughlin, *J. Chem. Phys.* **55**:3706 (1971).
11. D. Levesque, L. Verlet, and J. Kürkijarvi, *Phys. Rev.* **7**:1690 (1973).
12. D. J. Evans and W. B. Streett, *Mol. Phys.* **36**:161 (1978).
13. D. Levesque and L. Verlet, *Phys. Rev.* **2**:2514 (1970).
14. J. P. J. Michels and N. J. Trappeniers, *Physica* **90A**:179 (1978).
15. K. C. Mo, and K. E. Starling, private communication (1976).
16. J. O. Hirschfelder, J. O. Curtiss, and R. B. Bird, *Molecular Theory of Gases and Liquids* (Wiley, New York, 1965), p. 538.
17. A. L. Gosman, R. D. McCarty, and J. G. Hust, *Thermodynamic Properties of Argon from the Triple Point to 300 K at Pressures to 1000 Atmospheres* (NBS Reference Data Series 27, 1969).
18. C. H. Twu, L. L. Lee, and K. E. Starling, *Fluid Phase Equilibria* **4**:35 (1980).
19. W. M. Haynes, *Physica* **67**:440 (1973).
20. J. A. Gracki, G. P. Flynn, and J. Ross, *J. Chem. Phys.* **51**:3856 (1969).
21. A. Michels, A. Botzen, and W. Schuurman, *Physica* **20**:1141 (1954).
22. R. DiPippo and J. Kestin, *Proc. 4th Symp. Thermophys Properties* (ASME, New York, 1968), p. 304.
23. G. P. Flynn, R. V. Hanks, N. A. Lemaire, and J. Ross, *J. Chem. Phys.* **38**:154 (1963).
24. J. Kestin, B. Paykoc, and J. V. Sengers, *Physica,* **54**:1 (1971).
25. J. Kestin, S. T. Ro, and W. A. Wakeham, *J. Chem. Phys.* **56**:4119 (1972).
26. F. A. Guevara, B. B. McInteer, and W. E. Wageman, *Phys. Fluids* **12**:2493 (1969).
27. J. Hellemans, H. Zink, and O. Van Paemel, *Physica* **46**:395 (1970).
28. E. G. Reynes and G. Thodos, *Physica* **30**:1529 (1964).
29. J. Kestin and W. Leidenfrost, *Physica,* **25**:1033 (1969).
30. Y. Saji and S. Kobayasi, *Cryogenics* **4**:139 (1964).
31. V. A. Van Itterbeek, and O. Van Paemel. *Physica,* **8**:133 (1941).
32. J. P. Boon, J. C. Legros, and G. Thomaes, *Physica* **33**:547 (1967).
33. J. C. Legros and G. Thomaes, *Physica* **31**:703 (1965).
34. A. Michels, J. V. Sengers, and L. J. M. Van de Klundert, *Physica* **29**:149 (1963).
35. B. Le Neindre, R. Tufeu, P. Bury, P. Johannin, and B. Vodar, *Thermal Conductivity Proc. Eighth Conf.* (Plenum, New York, 1969), pp. 75–95.
36. J. R. Moszynski and B. P. Singh, *Proc. 6th Symp. Thermophys. Properties* (ASME, New York, 1973), p. 22.
37. J. Kestin and W. Wakeham, *Proc. 5th Symp. Thermophys. Properties* (ASME, New York, 1970), p. 55.
38. H. Ziebland and J. T. A. Burton, *Br. J. Appl. Phys.* **9**:52 (1958).
39. H. J. M. Hanley, R. D. McCarty and W. M. Haynes, *The Viscosity and Thermal Conductivity Coefficients for Dense Gaseous and Liquid Argon, Krypton, Xenon, Nitrogen and Oxygen, J. Phys. Chem. Ref. Data* **3**(4): 979 (1974).
40. C. Y. Ho, R. M. Powell, and P. E. Liley, *Thermal Conductivity of Selected Materials* (NBS Reference Data Series 16, 1968).
41. J. Naghizadeh and S. A. Rice. *J. Chem. Phys.* **36**:2710 (1962).